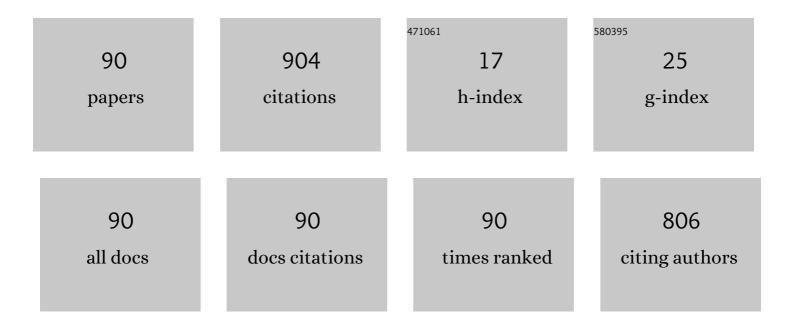
## Damiano Giubertoni

List of Publications by Year in descending order

Source: https://exaly.com/author-pdf/1531970/publications.pdf Version: 2024-02-01



#	Article	IF	CITATIONS
1	Transient enhanced diffusion of arsenic in silicon. Journal of Applied Physics, 2003, 94, 4950.	1.1	54
2	Depth profile characterization of ultra shallow junction implants. Analytical and Bioanalytical Chemistry, 2010, 396, 2825-2832.	1.9	50
3	Investigation on indium diffusion in silicon. Journal of Applied Physics, 2002, 92, 1361-1366.	1.1	48
4	P implantation into preamorphized germanium and subsequent annealing: Solid phase epitaxial regrowth, P diffusion, and activation. Journal of Vacuum Science & Technology B, 2008, 26, 430-434.	1.3	39
5	Deactivation of ultrashallow boron implants in preamorphized silicon after nonmelt laser annealing with multiple scans. Applied Physics Letters, 2006, 89, 192105.	1.5	35
6	Combined evaluation of grazing incidence X-ray fluorescence and X-ray reflectivity data for improved profiling of ultra-shallow depth distributions. Spectrochimica Acta, Part B: Atomic Spectroscopy, 2014, 99, 121-128.	1.5	32
7	Arsenic uphill diffusion during shallow junction formation. Journal of Applied Physics, 2006, 99, 113508.	1.1	31
8	Hydrogen diffusion inGaAs1â^'xNx. Physical Review B, 2009, 80, .	1.1	26
9	Nondestructive dose determination and depth profiling of arsenic ultrashallow junctions with total reflection X-ray fluorescence analysis compared to dynamic secondary ion mass spectrometry. Spectrochimica Acta, Part B: Atomic Spectroscopy, 2004, 59, 1243-1249.	1.5	23
10	Vacancy-engineering implants for high boron activation in silicon on insulator. Applied Physics Letters, 2006, 88, 082112.	1.5	23
11	Electrical activation of solid-phase epitaxially regrown ultra-low energy boron implants in Ge preamorphised silicon and SOI. Nuclear Instruments & Methods in Physics Research B, 2005, 237, 107-112.	0.6	22
12	Interphase exchange coupling in Feâ^•Sm–Co bilayers with gradient Fe thickness. Journal of Applied Physics, 2005, 98, 063908.	1.1	22
13	Diffusion and electrical activation of indium in silicon. Journal of Applied Physics, 2003, 93, 9773-9782.	1.1	21
14	Diffusion and activation of ultrashallow B implants in silicon on insulator: End-of-range defect dissolution and the buried Siâ^•SiO2 interface. Applied Physics Letters, 2006, 89, 042111.	1.5	20
15	Comparison between the SIMS and MEIS techniques for the characterization of ultra shallow arsenic implants. Applied Surface Science, 2006, 252, 7214-7217.	3.1	18
16	Correlation of local structure and electrical activation in arsenic ultrashallow junctions in silicon. Journal of Applied Physics, 2008, 104, .	1.1	18
17	Quantitative depth profiling of boron and arsenic ultra low energy implants by pulsed rf-GD-ToFMS. Journal of Analytical Atomic Spectrometry, 2011, 26, 542-549.	1.6	18
18	Correlation between silicon-nitride film stress and composition: XPS and SIMS analyses. Surface and Interface Analysis, 2006, 38, 723-726.	0.8	16

#	Article	IF	CITATIONS
19	Grazing incidence x-ray fluorescence and secondary ion mass spectrometry combined approach for the characterization of ultrashallow arsenic distribution in silicon. Journal of Vacuum Science and Technology B:Nanotechnology and Microelectronics, 2010, 28, C1C59-C1C64.	0.6	16
20	Quantitative determination of the dopant distribution in Si ultrashallow junctions by tilted sample annular dark field scanning transmission electron microscopy. Applied Physics Letters, 2008, 92, 261907.	1.5	15
21	Initial reactions in Ti–Si bilayers: New indications from in situ measurements. Journal of Applied Physics, 2001, 89, 6079-6084.	1.1	14
22	Boron ultra low energy SIMS depth profiling improved by rotating stage. Applied Surface Science, 2006, 252, 7315-7317.	3.1	14
23	Boron deactivation in preamorphized silicon on insulator: Efficiency of the buried oxide as an interstitial sink. Applied Physics Letters, 2007, 91, .	1.5	14
24	Effect of hydrogen incorporation temperature inin plane-engineered GaAsNâ^•GaAsN:H heterostructures. Applied Physics Letters, 2008, 92, 221901.	1.5	14
25	A new spectrometer for grazing incidence X-ray fluorescence for the characterization of Arsenic implants and Hf based high-k layers. Spectrochimica Acta, Part B: Atomic Spectroscopy, 2010, 65, 429-433.	1.5	14
26	Binder-free nanostructured germanium anode for high resilience lithium-ion battery. Electrochimica Acta, 2022, 411, 139832.	2.6	14
27	Topography induced by sputtering in a magnetic sector instrument: an AFM and SEM study. Applied Surface Science, 2004, 238, 24-28.	3.1	13
28	D-SIMS and ToF-SIMS quantitative depth profiles comparison on ultra thin oxynitrides. Applied Surface Science, 2003, 203-204, 281-284.	3.1	12
29	xmins:mmi="http://www.w3.org/1998/Wath/Wath/WathWi_display="inline"> <mmi:msub><mmi:mrow /&gt;<mml:mi>x</mml:mi>Ga<mml:math xmlns:mml="http://www.w3.org/1998/Math/MathML" display="inline"&gt;<mml:msub><mml:mrow /&gt;<mml:mrow><mml:mn>1</mml:mn><mml:mo>â^</mml:mo><mml:mi>x</mml:mi></mml:mrow><td>&gt; <td>ath&gt;N _</td></td></mml:mrow </mml:msub></mml:math </mmi:mrow </mmi:msub>	> <td>ath&gt;N _</td>	ath>N _

#	Article	IF	CITATIONS
37	Nitrogen Implantation and Diffusion in Crystalline Germanium: Implantation Energy, Temperature and Ge Surface Protection Dependence. ECS Journal of Solid State Science and Technology, 2012, 1, P315-P319.	0.9	8
38	Nanofabrication of self-organized periodic ripples by ion beam sputtering. Microelectronic Engineering, 2016, 155, 50-54.	1.1	8
39	Bimodal Approach for Noise Figures of Merit Evaluation in Quantum-Limited Josephson Traveling Wave Parametric Amplifiers. IEEE Transactions on Applied Superconductivity, 2022, 32, 1-6.	1.1	8
40	Investigation of C49–C54 TiSi2 transformation kinetics. Microelectronic Engineering, 2000, 50, 153-158.	1.1	7
41	Ultralow energy boron implants in silicon characterization by nonoxidizing secondary ion mass spectrometry analysis and soft x-ray grazing incidence x-ray fluorescence techniques. Journal of Vacuum Science and Technology B:Nanotechnology and Microelectronics, 2010, 28, C1C84-C1C89.	0.6	7
42	High performance n+/p and p+/n germanium diodes at low-temperature activation annealing. Microelectronic Engineering, 2011, 88, 254-261.	1.1	7
43	Surface proximity and boron concentration effects on end-of-range defect formation during nonmelt laser annealing. Applied Physics Letters, 2008, 92, .	1.5	6
44	Non-melting annealing of silicon by CO2 laser. Thin Solid Films, 2010, 518, 2551-2554.	0.8	6
45	Deactivation of submelt laser annealed arsenic ultrashallow junctions in silicon during subsequent thermal treatment. Journal of Vacuum Science and Technology B:Nanotechnology and Microelectronics, 2010, 28, C1B1-C1B5.	0.6	6
46	Short-term and long-term RSF repeatability for CAMECA SC-Ultra SIMS measurements. Applied Surface Science, 2004, 231-232, 768-771.	3.1	5
47	Influence of changes in the resistivity of the sample surface on ultra-shallow SIMS profiles for arsenic. Applied Surface Science, 2006, 252, 7286-7289.	3.1	5
48	Differential Hall characterisation of ultrashallow doping in advanced Si-based materials. Materials Science and Engineering B: Solid-State Materials for Advanced Technology, 2008, 154-155, 229-233.	1.7	5
49	Formation of arsenolite crystals at room temperature after very high dose arsenic implantation in silicon. Applied Physics Letters, 2012, 101, .	1.5	5
50	Formation of arsenic rich silicon oxide under plasma immersion ion implantation and laser annealing. AIP Conference Proceedings, 2012, , .	0.3	5
51	The role of incidence angle in the morphology evolution of Ge surfaces irradiated by medium-energy Au ions. Journal of Physics Condensed Matter, 2018, 30, 324001.	0.7	5
52	Hydrogen as a probe of the electronic properties of (InGa)(AsN)/GaAs heterostructures. Solid-State Electronics, 2003, 47, 447-453.	0.8	4
53	Optimization of secondary ion mass spectrometry ultra-shallow boron profiles using an oblique incidence O[sub 2][sup +] beam. Journal of Vacuum Science & Technology an Official Journal of the American Vacuum Society B, Microelectronics Processing and Phenomena, 2004, 22, 336.	1.6	4
54	Effect of buried Siâ^•SiO[sub 2] interface on dopant and defect evolution in preamorphizing implant ultrashallow junction. Journal of Vacuum Science & Technology B, 2006, 24, 442.	1.3	4

#	Article	IF	CITATIONS
55	Nonconventional flash annealing on shallow indium implants in silicon. Journal of Vacuum Science & Technology B, 2006, 24, 473.	1.3	4
56	Deuterium depth profile quantification in a ASDEX Upgrade divertor tile using secondary ion mass spectrometry. Applied Surface Science, 2014, 315, 459-466.	3.1	4
57	Surface evolution of very high dose arsenic implants in silicon formed by plasma immersion ion implantation – a long term study. Physica Status Solidi C: Current Topics in Solid State Physics, 2014, 11, 28-31.	0.8	4
58	Peculiarities of the hydrogenated In(AsN) alloy. Semiconductor Science and Technology, 2015, 30, 105030.	1.0	4
59	Evolution of arsenic in high fluence plasma immersion ion implanted silicon: Behavior of the as-implanted surface. Applied Surface Science, 2015, 355, 792-799.	3.1	4
60	H-tailored surface conductivity in narrow band gap In(AsN). Applied Physics Letters, 2015, 106, .	1.5	4
61	Junction Stability of B Doped Layers in SOI Formed with Optimized Vacancy Engineering Implants. AIP Conference Proceedings, 2006, , .	0.3	3
62	GIXRF In The Soft X-Ray Range Used For The Characterization Of Ultra Shallow Junctions. , 2009, , .		3
63	Characterisation of ultra-shallow disorder profiles and dielectric functions in ion implanted Si. Thin Solid Films, 2011, 519, 2847-2851.	0.8	3
64	Solid phase epitaxial re-growth of Sn ion implanted germanium thin films. AIP Conference Proceedings, 2012, , .	0.3	3
65	Development of nano-roughness under SIMS ion sputtering of germanium surfaces. Surface and Interface Analysis, 2013, 45, 409-412.	0.8	3
66	The interaction between Xe and F in Si (100) pre-amorphised with 20keV Xe and implanted with low energy BF2. Materials Science and Engineering B: Solid-State Materials for Advanced Technology, 2004, 114-115, 198-202.	1.7	2
67	Understanding the role of buried Si/SiO2 interface on dopant and defect evolution in PAI USJ. Materials Science and Engineering B: Solid-State Materials for Advanced Technology, 2005, 124-125, 215-218.	1.7	2
68	Thermodynamical analysis of abrupt interfaces of InGaP/GaAs and GaAs/InGaP heterostructures. Crystal Research and Technology, 2005, 40, 982-986.	0.6	2
69	Multi-technique characterization of arsenic ultra shallow junctions in silicon within the ANNA consortium. , 2009, , .		2
70	Arsenic redistribution after solid phase epitaxial regrowth of shallow pre-amorphized silicon layers. AIP Conference Proceedings, 2012, , .	0.3	2
71	Quality management system and accreditation of measurements in a surface science laboratory: the case study of MiNALab. Surface and Interface Analysis, 2014, 46, 927-930.	0.8	2
72	On an improved boron segregation calibration from a particularly sensitive power MOS process. Physica Status Solidi C: Current Topics in Solid State Physics, 2014, 11, 12-15.	0.8	2

DAMIANO GIUBERTONI

#	Article	IF	CITATIONS
73	Omnidirectional and broadband photon harvesting in self-organized Ge columnar nanovoids. Nanotechnology, 2022, 33, 305304.	1.3	2
74	XPS and SIMS depth profiling of chlorine in high-temperature oxynitrides. Surface and Interface Analysis, 2002, 34, 271-275.	0.8	1
75	Indium in silicon: a study on diffusion and electrical activation Materials Research Society Symposia Proceedings, 2003, 765, 1.	0.1	1
76	In-depth analysis of the interfaces in InGaP/GaAs heterosystems. EPJ Applied Physics, 2004, 27, 379-383.	0.3	1
77	Sample holder implement for very small samples on SC-ultra SIMS instrument. Applied Surface Science, 2004, 231-232, 959-961.	3.1	1
78	Role of the Siâ^•SiO2 interface during dopant diffusion in thin silicon on insulator layers. Journal of Applied Physics, 2006, 100, 096112.	1.1	1
79	Effect of B dose and Ge preamorphization energy on the electrical and structural properties of ultrashallow junctions in silicon-on-insulator. Materials Research Society Symposia Proceedings, 2006, 912, 1.	0.1	1
80	Si Ultra Shallow Junctions Dopant Profiling with ADF-STEM. Materials Research Society Symposia Proceedings, 2007, 1026, 1.	0.1	1
81	Calibration correction of ultra low energy SIMS profiles based on MEIS analysis of shallow arsenic implants in silicon. Surface and Interface Analysis, 2013, 45, 413-416.	0.8	1
82	Preface for Proceedings of SIMS XVIII, Riva del Garda, Italy, 2011. Surface and Interface Analysis, 2013, 45, 1-2.	0.8	1
83	Development of nanotopography during SIMS characterization of thin films of Ge1â^'Sn alloy. Applied Surface Science, 2015, 356, 422-428.	3.1	1
84	Boron pile-up phenomena during ultra shallow junction formation. , 2007, , .		0
85	Characterization of junction activation and deactivation using non-equilibrium annealing: Solid phase epitaxy, spike annealing, laser annealing instructions for. , 2009, , .		Ο
86	Tuning of the optical properties of In-rich In[sub x]Ga[sub 1â^'x]N (x=0.82â^'0.49) alloys by light-ion irradiation at low energy. , 2013, , .		0
87	Observation of point defect injection from electrical deactivation of arsenic ultraâ€shallow distributions formed by ultraâ€low energy ion implantation and laser subâ€melt annealing. Physica Status Solidi C: Current Topics in Solid State Physics, 2014, 11, 16-19.	0.8	Ο
88	Silicon defects characterization for low temperature ion implantation and RTA process. Nuclear Instruments & Methods in Physics Research B, 2015, 365, 283-287.	0.6	0
89	Selective Effects of the Host Matrix in Hydrogenated InGaAsN Alloys: Toward an Integrated Matrix/Defect Engineering Paradigm. Advanced Functional Materials, 2022, 32, 2108862.	7.8	0
90	Porous Germanium Anode for Li-Ion Batteries. ECS Meeting Abstracts, 2019, , .	0.0	0